Genes & Cancer
2(1) 10–19

DOI: 10.1177/1947601911402682
http://ganc.sagepub.com

A Role for PML in Innate Immunity

Andrea Lunardi[1], Mirella Gaboli[2,3], Marco Giorgio[2,4], Roberta Rivi[2], Anne Bygrave[5,6], Michael Antoniou[7,8], Dubravka Drabek[5,9], Elaine Dzierzak[5,10], Marta Fagioli[11], Leonardo Salmena[1], Marina Botto[12], Carlos Cordon-Cardo[2,13], Lucio Luzzatto[2,14], Pier Giuseppe Pelicci[4], Frank Grosveld[5,9], and Pier Paolo Pandolfi[1,2]

Submitted 30-Jan-2011; accepted 09-Feb-2011

Abstract

The promyelocytic leukemia gene (*PML*) of acute promyelocytic leukemia is an established tumor suppressor gene with critical functions in growth suppression, induction of apoptosis, and cellular senescence. Interestingly, although less studied, PML seems to play a key role also in immune response to viral infection. Herein, we report that *Pml*$^{-/-}$ mice spontaneously develop an atypical invasive and lethal granulomatous lesion known as botryomycosis (BTM). In *Pml*$^{-/-}$ mice, BTM is the result of impaired function of macrophages, whereby they fail to become activated and are thus unable to clear pathogenic microorganisms. Accordingly, *Pml*$^{-/-}$ mice are resistant to lipopolysaccharide (LPS)–induced septic shock as a result of an ineffective production of cytokines and chemokines, suggesting a role for PML in the innate immune Toll-like receptor (TLR)/NF-κB prosurvival pathway. These results not only shed light on a new fundamental function of PML in innate immunity, but they also point to a proto-oncogenic role for PML in certain cellular and pathological contexts.

Keywords

PML, innate immunity, botryomycosis

Introduction

PML, a gene that is involved in the t(15;17) chromosomal translocation of acute promyelocytic leukemia (APL), encodes a RING–B-box–coiled-coil protein implicated in fundamental cellular processes such as genomic stability, apoptosis, cellular proliferation, and senescence.[1,2] Although cytosolic PML plays an important role in the TGF-β pathway and apoptosis,[3] PML nuclear body (PML-NB)–associated PML is responsible for the regulation of many different cellular functions.[4,5] An increasing body of evidence suggests that PML and PML-NBs operate as a hub where different pathways converge for positive or negative regulation. For instance, PML is involved in p53 activation, Rb function and PTEN localization under stress conditions, and also in the repression of the PI3K/Akt pathway through inhibition of the nuclear activity of Akt and by nuclear relocalization of mTOR.[6-11] Importantly, the tumor suppressor role of PML is reinforced by the frequent loss of this protein and its subnuclear domains in leukemias and solid tumors.[12] Furthermore, the growth-suppressive functions of PML have been recently implicated in neural and hematopoietic stem cell functions.[13,14] Interestingly, however, recent reports strengthen the notion that deregulation of PML may also play a crucial role in innate and adaptive immunity.[15-17] During viral infections type I and II interferons (IFNs) bind IFN-stimulated response element (ISRE) and INF-γ activation site (GAS) elements on the PML and SP100 promoters, thereby greatly inducing their transcription. The consequence of such infections is a greater number and size of NBs and a NB-dependent transcriptional

[1]Cancer Genetics Program, Beth Israel Deaconess Cancer Center, Department of Medicine and Pathology, Beth Israel Deaconess Medical Center, Harvard Medical School, Boston, MA, USA.
[2]Department of Pathology and Human Genetics, Molecular Biology and Cancer Genetics Program Sloan-Kettering Institute, Memorial Sloan-Kettering Cancer Center, New York, USA.
[3]Department of Pediatrics, University Hospital and University of Salamanca, Salamanca, Spain.
[4]Department of Experimental Oncology, European Institute of Oncology, Milan, Italy.
[5]Laboratory of Gene Structure and Expression, National Institute for Medical Research, Mill Hill, UK.
[6]Molecular Genetics and Rheumatology Section, Faculty of Medicine, Imperial College, London, UK.
[7]Department of Experimental Pathology, Guy's Hospital, London, UK.
[8]Gene expression and Therapy Group King's College London School of Medicine Department of Medical and Molecular Genetics, London UK.
[9]Erasmus Medical Center, Department of Cell Biology, Cancer Genomics Center, Rotterdam, The Netherlands.
[10]Erasmus Medical Center, Department of Cell Biology, Erasmus MC Stem Cell Institute, Rotterdam, The Netherlands.
[11]Sezione di Medicina Interna e Scienze Oncologiche, Università di Perugia, Italy.
[12]Imperial College Rheumathology Section Eric Baywaters Centre Faculty of Medicine Imperial College, Hammersmith Campus, London, UK.
[13]Department of Pathology, Herbert Irving Comprehensive Cancer Center, Columbia University Medical Center, New York, USA.
[14]Istituto Toscano Tumori Florence, Italy.

Corresponding Author:
Pier Paolo Pandolfi, Cancer Genetics Program, Beth Israel Deaconess Cancer Center, Department of Medicine and Pathology, Beth Israel Deaconess Medical Center, Harvard Medical School, CLS0424 3 Blackfan Circle, Boston, MA 02115
Email: ppandolf@bidmc.harvard.edu

program to repress viral genes expression.[15] If this represents only a small part of the IFN-mediated viral response program, the ability of different classes of viruses to disrupt PML-NBs in the first phase of infection provides convincing evidence that a key function of PML and PML-NBs is the mediation of intrinsic antiviral defense.[18]

Innate immunity is essential for the clearance of bacterial infections. Recognition of fragments of pathogenic microbes like LPS, a lipopolysaccharide commonly expressed in Gram-negative bacterial membrane, by the Toll-like receptors (TLRs) class of molecules is a cornerstone of innate immunity.[19] Ligand-dependent dimerization of TLRs is the trigger for potent activation of the NF-κB pathway that in turn leads to a rapid induction of prosurvival genes (Bcl-2, c-FLIP, IAP, and TRAF molecules) and a wide variety of proinflammatory cytokines and chemokines (IL6, IL8, IL10, IL23, IL1α, IL1β, and TNF-α).[20]

Although innate immunity plays a key role in the defense against various invading pathogens, a growing amount of evidence describes a tight relationship between inflammation, tumorigenesis, and tumor progression. Numerous recent studies have clearly demonstrated that bacterial- and viral-induced inflammatory processes as well as chronic inflammation due to tissue injury can mediate tumorigenesis.[21-25] Infiltrated inflammatory cells, primarily macrophages, through the release of cytokines and chemokines may be responsible for the activation of TLR/NF-κB pathway in the cancer cells, thereby promoting cell survival and chemoresistance, in addition to activation of neoangiogenesis by VEGF production and extracellular matrix breakdown by the release of extracellular matrix proteases.[26]

Herein, we describe an aberrant immune response of *Pml*$^{-/-}$ mice to spontaneous and experimental bacterial infections. We find that *Pml*$^{-/-}$ macrophages are dysfunctional. Importantly, *Pml*$^{-/-}$ mice are resistant to the acute LPS-mediated lethality observed in wild-type mice, while *Pml*$^{-/-}$ cells display a markedly reduced IL6 response compared to wild-type controls after LPS stimulation. Taken together, our data not only demonstrate an important role for PML in the innate immunity and acute inflammatory response but also suggest a more general function of PML in the TLR/NF-κB pathway, shedding light on a possible proto-oncogenic role of this gene in the context of chronic inflammation-driven tumor development.

Results

Spontaneous botryomycosis and abnormal immunohistopathological features of infected Pml$^{-/-}$ *mice*. *Pml*$^{-/-}$ animals are extremely prone to develop spontaneous infection when housed in a non-pathogen-free area. Although septicemia and severely destructive and ulcerating skin infections were documented in some cases, the majority of *Pml*$^{-/-}$ mice succumb to an unusual tumor-like lesion that resembles what has been previously described as "botryomycosis (BTM)" (Fig. 1A and 1B). BTM is a chronic granulomatous lesion attributed in humans to *Actinomycetes* or *Staphylococcus aureus* and is thought to be invariably associated with an immunocompromised state of the host organism. In fact, it should be noted that the lesion is not transmissible from animal to animal or from man to animal.[27,28] Neither the pathogenic mechanism, nor the immunocompromising condition, or the predisposing genetic defect that causes the host to respond to an infection by producing chronically proliferating and invasive granulomas are currently clear. Thirty percent of *Pml*$^{-/-}$ mice developed spontaneous BTM by the first year of age (Fig. 1A and 1B). One hundred percent of these animals showed macroscopic or microscopic BTM lesions by 18 months. Although classic BTM presents in the head and neck region, several *Pml*$^{-/-}$ mice were affected in the kidney, the preputial glands, or the ovary.

Postmortem characterization of infected *Pml*$^{-/-}$ animals revealed additional striking features, including infections other than BTM: 1) proliferation of plasma cells that were massively infiltrated into the BTM lesion (Fig. 1C) and organs to which the infection apparently had not overtly spread (lungs and kidneys were frequently infiltrated; not shown). The site of infection was surrounded by large hyperplastic lymph nodes characterized by a dramatic proliferation of plasma cells (Fig. 1E). Plasma cell proliferation was not monoclonal in origin as revealed by immunohistochemical staining for κδ immunoglobulin light chain of the proliferating plasma cells. Plasma cell proliferation was accompanied by an increase of IgG1A in the serum of the infected *Pml*$^{-/-}$ mice as measured by ELISA, while uninfected *Pml*$^{-/-}$ mice showed only a 50% reduction of circulating IgE when compared to uninfected wild-type controls of the same sex and age. 2) Hyperleukocytosis in the peripheral blood with values $>2 \times 10^4$ cells/μL; 3) extramedullary hemopoiesis in the liver and the spleen accompanied by massive splenomegaly with marked hyperplasia of the white pulp was also invariably observed (Fig. 1G-I); 4) the presence of abnormal macrophages demonstrating lipochrome granulation (Fig. 1F). Such abnormal macrophages are diagnostic of familial syndromes including the various forms of chronic granulomatous disease (CGD), characterized by altered macrophage function, and are thought to represent engulfed macrophages.[29-31] 5) The lung was frequently damaged irrespective of the primary site of infection and the type of infection (Fig. 1J). Areas of emphysema and atelectasis were also observed. The alveolar wall was thickened by an infiltrate of mononuclear cells, plasma cells, and the deposition of fibrous material. No microabscesses were identifiable, and the lung itself was never found to be involved as the primary site of infection. Interestingly, damaged lungs were also observed in 30% of apparently uninfected *Pml*$^{-/-}$ mice. 6) When the salivary gland was the primary site of infection (almost 70% of

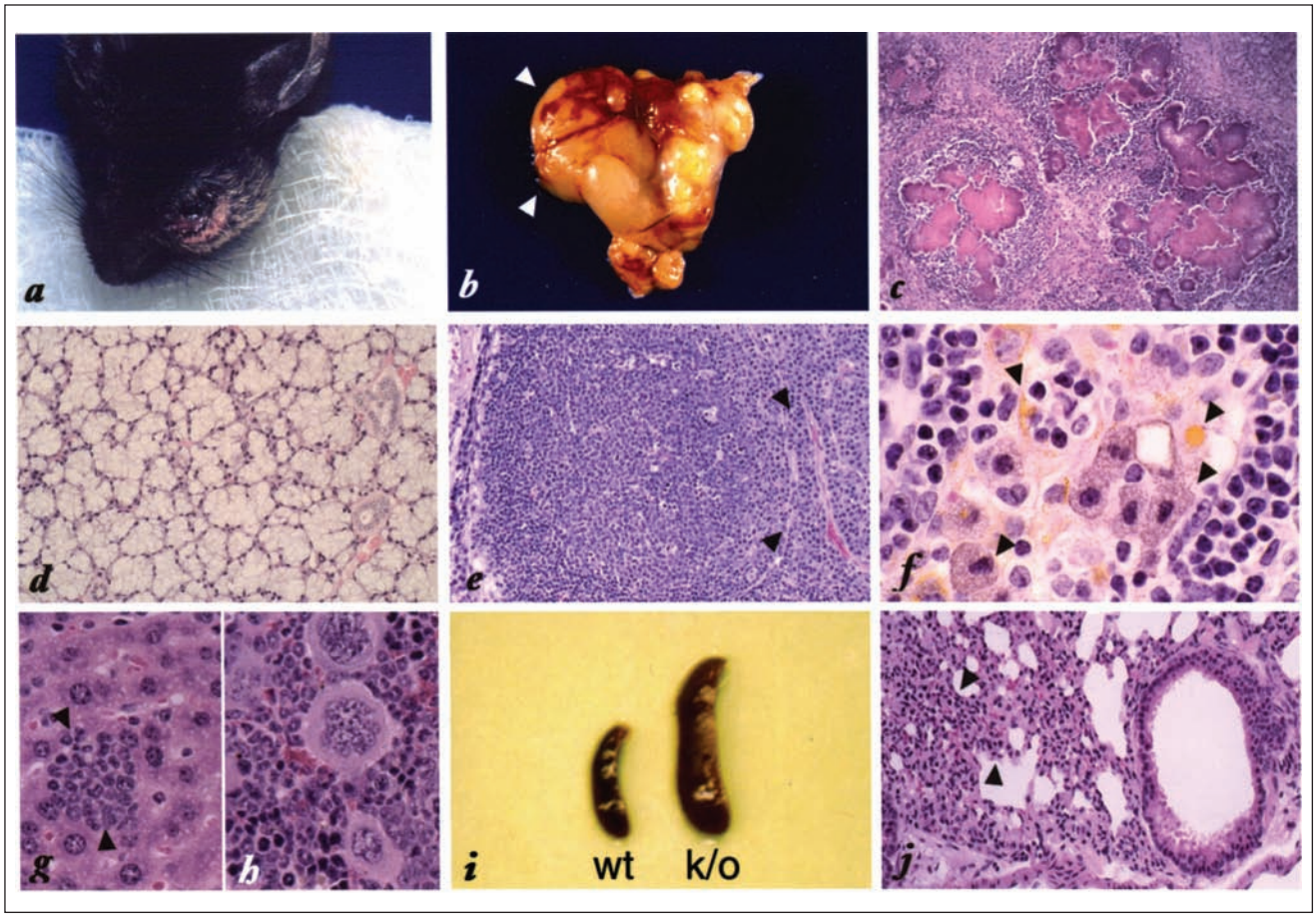

Figure 1. Spontaneous botryomycosis in *Pml*$^{-/-}$ mice. Pathological features of spontaneous botryomicosis affecting *Pml*$^{-/-}$ mutants. (**A**) Botryomycosis in the salivary gland. The left glandular lobe is almost completely replaced by the lesion; overt hyperplasia of the salivary gland is visible (**B, D**) and also involves the right lobe as indicated by the arrowheads (**B**). Magnification of the granulomatous area is shown (**C**): pink cauliflower-like structure consisting of bacterial and proteinaceous material is surrounded by granulocytes and macrophages but mainly by plasma cells. Plasma cell infiltration also affected organs not directly involved in the infection such as the lung and kidney (not shown). (**E**) Plasma cell proliferation, as indicated by the arrowheads, massively involves the surrounding lymph nodes. (**F**) Lipochrome granulation of macrophages surrounding the lesion (arrowheads). These cells were also infiltrating the lymph nodes and the lungs (not shown). (**G**) Extramedullary hemopoiesis in the liver. The arrowheads indicate islands of hemopoiesis. (**H**) Extramedullary hemopoiesis in the spleen of infected *Pml*$^{-/-}$ mice (many megakaryocytes are visible), accompanied by massive splenomegaly (**I**). (**J**) Interstitial infiltrates of mononuclear cells in the lung. The arrowheads indicate a thickened alveolar wall. Atelectasis of the lung parenchyma is also visible. This picture is frequently observed in apparently uninfected mice.

cases), it showed a marked acinar hyperplasia with clear signs of dysplasia in some areas (Fig. 1D).

The almost complete penetrance of this rare and unusual infectious lesion in our animal house prompted us to identify the causative microorganism. In asepsis, we biopsied 2 cases in which the lesion had a facial presentation and looked for the presence of either aerobial or anaerobial bacteria or fungi. *Staphylococcus aureus* was the prominent bacterial species isolated, although *Escherichia coli*, *Enterococcus*, *Klebsiella pneumoniae*, and *Proteus mirabilis* were also reported. Neither actinomyces nor fungi were isolated from the lesion. It is noteworthy that all the bacterial strains found in the BTM infection are normally found in the oral cavity of the mouse. All the bacteria isolated were sensitive to all the antibiotics tested including ampicillin. The isolation of *Staphylococcus aureus* from the lesion is in agreement with the Gram-positive staining pattern observed in part of the central region of the abscess.

Hyperproliferative and impaired response to local and systemic experimental infection with Staphylococcus aureus and Listeria monocytogenes in Pml$^{-/-}$ *mutants*. In an attempt to reproduce the histopathological findings observed in the *Pml*$^{-/-}$ animals, we tested their responses to experimentally induced systemic and local bacterial infections. We first determined the minimum lethal intraperitoneal dose of *Staphylococcus aureus* for the 129Sv control mice, approximately 5×10^8 cfu, and injected *Pml*$^{-/-}$ mice and

controls with this dose. The postmortem analysis revealed a consistent qualitative difference between the 2 groups. *Pml*$^{-/-}$ mice were characterized by the following: 1) heavily damaged and congested lungs and areas of emphysema and atelectasis were frequently observed, and the alveolar wall was thickened by an infiltrate of mononuclear cells (Fig. 2A); 2) a marked proliferation of plasma cells in several organs not observed in control animals. In some cases, this monomorphic cellular population entirely replaced the red pulp of the spleen, causing complete subversion of its normal structure (Fig. 2B). 3) Disseminated abscesses affecting almost all organs, including the brain, accompanied by overt suppurative peritonitis (data not shown); 4) again, many pigmented histiocytes were observed in the proximity of the abscesses, spleen, and lymph nodes (Fig. 2B). Wild-type mice, on the contrary, consistently died from renal or heart failure due to abscess formation and infraction only localized in these organs (data not shown).

The response of *Pml*$^{-/-}$ mice to localized injection of bacteria was tested by inoculating 5×10^7 cfu of *Staphylococcus aureus* into the left lobe of the submandibular salivary gland of *Pml*$^{-/-}$ and control animals. Mice were followed for 10 days and then sacrificed for postmortem analysis. Already after a few days, at clinical examination, the size of injected areas was overtly swollen in *Pml*$^{-/-}$ animals but not in the injected controls (Fig. 2C). The postmortem analysis confirmed this observation and revealed that the enlargement of the injected salivary gland lobe was due to a marked hyperplasia of the salivary gland itself and of lymph nodes with plasma cell, granulocyte, and mononuclear cell infiltration. Due to the presence of abnormal macrophages in the *Pml*$^{-/-}$ mice and in view of the specific up-regulation of PML expression by interferons, listeriosis of mice represented a preferred model.[32] Macrophages, in their resting state, are the major habitat for *Listeria monocytogenes*. Their functional activation by various cytokines including interferons, or microbial stimuli, converts these cells from being just the host of the pathogen into the main effectors of cell resistance.[33] *Pml*$^{-/-}$ and wild-type animals were injected with *Listeria monocytogenes* (1×10^4 cfu) and sacrificed after 6 days or analyzed as soon as spontaneous death occurred. The number of bacterial cfu from the spleen and liver homogenate was determined in 3 independent experiments. Four of 12 *Pml*$^{-/-}$ mice died spontaneously before day 6, whereas only one 129Sv control mouse died at that dose. In 6 of 12 *Pml*$^{-/-}$ mice, the colonies obtained were $>10^6$, both in the liver and in the spleen. In all 3 experiments, the number of *Listeria monocytogenes* colonies obtained from both the liver and spleen of the infected *Pml*$^{-/-}$ animals was 2 logarithms higher than from the controls (Fig. 2D).

Inefficient macrophage "activation" upon Listeria monocytogenes infection in Pml$^{-/-}$ *mutants*. The "activated" macrophage is the primary host cell mediating resistance to *Listeria monocytogenes*. Macrophage migration to the site of *Listeria* replication, activation, phagocytosis, and intracellular killing represents 4 different important mechanisms for the eradication of *Listeria*. We first examined whether the migration of macrophages into the peritoneal cavity is diminished in *Pml*$^{-/-}$ mice. The cell numbers of peritoneal exudate macrophages of untreated wild-type and *Pml*$^{-/-}$ mice 3 to 4 days after peritoneal injection with thioglycolate or proteose peptone were comparable, demonstrating that the migration of *Pml*$^{-/-}$ macrophages in the peritoneum was not impaired (data not shown). We next examined phagocytic activity of macrophages from wild-type and *Pml*$^{-/-}$ mice. Untreated resident macrophages were incubated with zymosan or red cells coated with antibodies in order to evaluate the phagocytosis mediated by the Fcγ receptors. Macrophages from both *Pml*$^{-/-}$ and control mice phagocytosed zymosan and coated red cells to a similar extent, suggesting that the phagocytic activity was not impaired (data not shown). Upon exposure to a microorganism or to various cytokines, untreated resident macrophages undergo dramatic functional and morphological changes and are then recognized as "activated." From the morphological point of view, the plasma membranes of activated macrophages become convoluted with ruffling and deep invaginations, and the cytoplasm markedly enlarges with the prominent appearance of numerous lysosomes.[34] Upon phagocytosis, lysosomes are almost immediately released into the phagosome to form phagolysosome, resulting in the killing and digestion of the phagocytosed microorganisms. We investigated whether there was any difference between *Pml*$^{-/-}$ and wild-type macrophage activation upon exposure to *Listeria monocytogenes*. Untreated wild-type and *Pml*$^{-/-}$ mice were inoculated intraperitoneally with *Listeria*. Fifteen minutes later, macrophages were harvested and then fixed, sectioned, and examined by electron microscopy (Fig. 2F-I). The vast majority of macrophages from wild-type mice showed the expected morphological features: convoluted plasma membrane with a nuclear to cytoplasmic ratio of <1 and the presence of >10 lysosomes per cell (76%) (Table 1). In contrast, *Pml*$^{-/-}$ macrophages did not show such changes. The majority of *Pml*$^{-/-}$ macrophages (75%) were smaller in size (nuclear to cytoplasmic ratio >1) with smooth plasma membranes and few or no lysosomes, even when phagocytosis was occurring (Fig. 2F-I and Table 1). These results indicate that *Pml* disruption impairs the activation capacity of macrophages, resulting in the *Listeria* killing defect observed *in vivo* in the *Pml*$^{-/-}$ mice.

While the mechanisms by which active macrophages kill intracellular pathogens are diverse and complex, a number of studies have demonstrated the importance of nitric oxide (NO) as an antimicrobial agent, although in some cases, the capacity to kill *Listeria* can be dramatically reduced even if

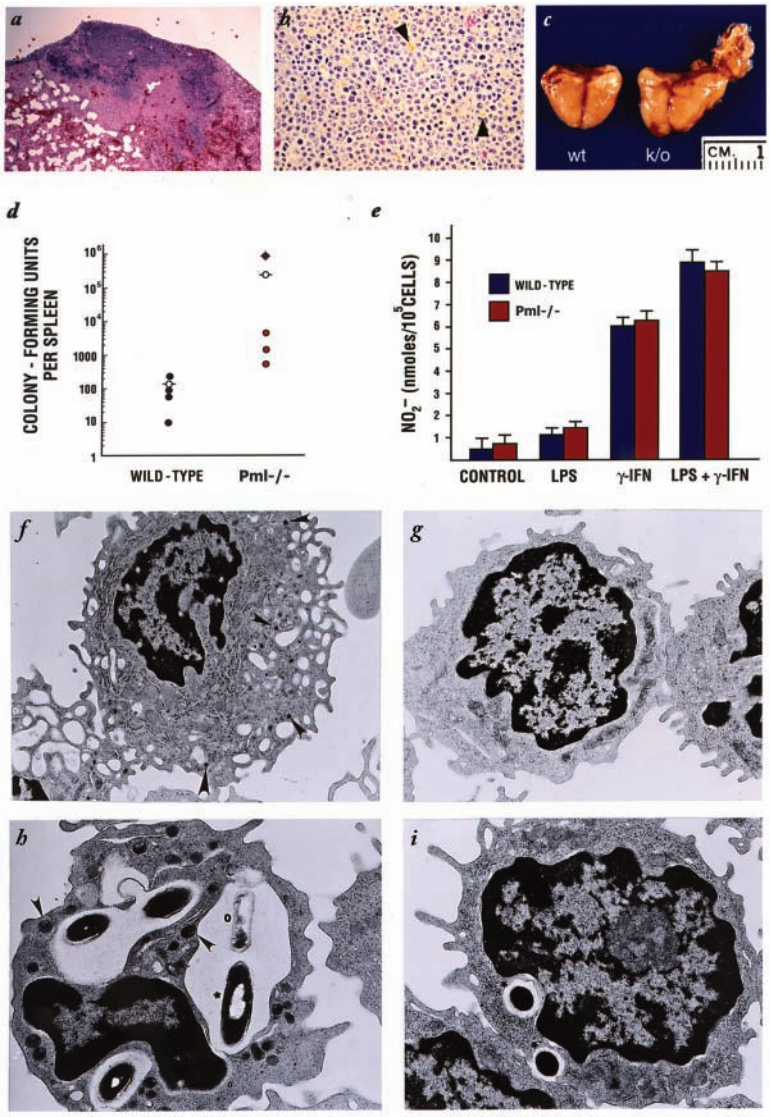

Figure 2. Aberrant response to infections and impaired macrophage function in *Pml*$^{-/-}$ mice. (**A**) Massive abscess and atelectasis due to hyperproliferative infiltration of the lung parenchyma in *Pml*$^{-/-}$ mice infected intraperitoneally with *Staphylococcus aureus*. Overt peritonitis in 4 of 8 *Pml*$^{-/-}$ mice was also observed. In control mice, abscesses were confined to the kidney and heart (not shown). In all infected *Pml*$^{-/-}$ mice, plasma cells and lipochrome macrophages (arrowheads) infiltrated the spleen and lymph nodes. In 3 cases, these cells completely replaced the red pulp of the spleen as shown (**B**). (**C**) Hyperplasia of the salivary gland in *Pml*$^{-/-}$ mice injected locally with *Staphylococcus aureus*. At postmortem analysis, the injected lobe of the salivary gland of all the *Pml*$^{-/-}$ was overtly swollen. The injected salivary gland of a representative *Pml*$^{-/-}$ mutant is shown on the right (k/o). Note the hyperplasia of the left lobe of the salivary gland itself and the hyperplasia of the surrounding lymph nodes that are fused to the lobe. On the left is an injected salivary gland from a control mouse. In this case, the only noticeable alteration is the fibrosis of the injected lobe. (**D**) *Pml*$^{-/-}$ mice show impaired response to *Listeria monocytogenes* infections. The number of *Listeria* colonies from the spleen of the first of 3 consecutive experiments performed with 4 *Pml*$^{-/-}$ and 4 wild-type animals is shown. The value obtained from one *Pml*$^{-/-}$ mutant, which in this experiment spontaneously died at day 5, is indicated by the crossed circle. The 2 mean values from the 2 groups are presented by the dashed open circles. The values obtained from the liver in 2 groups were comparable to the value obtained for the spleen (not shown). Two additional experiments on 8 *Pml*$^{-/-}$ and 8 wild-type mice, repeated using the same experimental conditions, showed virtually identical results (not shown). The mean values in the 3 experiments showed at least a 100-fold difference between the 2 groups. (**E**) Nitric oxide production by the *Pml*$^{-/-}$ macrophages. Resident untreated macrophages were collected from both wild-type and *Pml*$^{-/-}$ mice and cultured with or without 1,000 U/mL IFNγ, 100 ng/mL LPS, or both IFNγ and LPS for 48 hours. NO_2 concentration in the medium was measured with Griess reagent. The experiment shown represents triplicate measurements from the macrophage of 2 *Pml*$^{-/-}$ and 2 wild-type mice. Three independent experiments showed similar results. (**F-I**) Defective activation in *Pml*$^{-/-}$ macrophages is shown (**F**). Wild-type macrophage upon exposure to *Listeria*. The plasma membrane is convoluted with pronounced ruffling. The cytoplasm is large and contains numerous lysosomes as indicated by the arrowheads. (**G**) *Pml*$^{-/-}$ macrophages upon exposure to *Listeria*. The plasma membrane is smoother, and the cytoplasm is smaller with few or no lysosomes. (**H**) Phagocytosing wild-type macrophage. Phagolysosomes with phagocytosed *Listeria* and fusing lysosomes are clearly visible. The arrowheads indicate lysosomes ready to fuse to the endosome. The asterisk indicates a phagocytosed bacterium, and the open circle indicates a bacterium already partially digested. (**I**) Phagocytosing *Pml*$^{-/-}$ macrophage. Phagocytosed bacteria are in vacuoles (see asterisks), but no lysosomes are ready to fuse to them, nor does the macrophage seem to be activated. Magnifications are as follows: 4.400x (**F, G**) and 10.400x (**H, I**).

Table 1. Impaired *Pml*$^{-/-}$ Macrophage Activation upon *Listeria monocytogenes* Infection

	Lysosomes per cell (mean value)	Lysosomes in nonphagocitosing cell (mean value)	% of phagocitosing cells	Bacteria per cell (mean value)	% of bacteria not in endosomes	% of Mθ morphologically activated[a]
WT	16.2	17.5	62	2.1	7	76
Pml$^{-/-}$	7.8	7.4	25	2	25	25

Note: Total number of Mθ scored from 7 fields (3,000x-4,400x) in one electron microscopy section: wild-type (WT) = 21; *Pml*$^{-/-}$ = 24.
[a]Macrophages were considered activated when showing extensive ruffling of the plasma membrane and a reduced nucleus/cytoplasm ratio.

Table 2. Acute Septic Shock Response in *Pml*$^{-/-}$ and WT Mice to LPS Injection

	129Sv	129Sv-mixed	C57BL/6
WT	0/3	1/4	0/3
Pml$^{-/-}$	3/3	4/4	3/3

Note: *E. coli* LPS was injected intraperitoneally in 0.1 mL of sterile phosphate-buffered saline. The final result of the experiment (survival) was scored after 48 hours.

NO production is unaltered.[35] When untreated resident macrophages were cultured in the presence of IFNγ and LPS for 24 and 48 hours, the NO production was similar in *Pml*$^{-/-}$ and wild-type macrophage cultures (Fig. 2E). Furthermore, the reactive oxygen intermediate production from neutrophils evaluated by the NBT test was comparable between wild-type and *Pml*$^{-/-}$ mice. These results indicate that normal NO production is not sufficient for bactericidal activity and that Pml-dependent macrophage activation is essential to kill *Listeria monocytogenes*.

Impaired LPS response in Pml$^{-/-}$ *mice*. TLR-4 activation by LPS binding results in NF-κB–dependent induction of potent effector cytokines such as IL1 and TNF-α. Excessive production of cytokines and secondary mediators due to high levels of free LPS results in systemic vasodilation (hypotension), myocardial pump failure, and disseminated intravascular coagulation that in turn cause the multiorgan system failure referred to as septic shock syndrome. In order to determine whether the BTM phenotype observed in *Pml*$^{-/-}$ mice was attributable to an inefficient macrophage activation or to a more general dysfunction of the innate immune system and TLR/NF-κB pathway, we challenged wild-type and *Pml*$^{-/-}$ mice with bacterial LPS that have been previously reported to induce a fulminant hepatitis in mice. Wild-type mice injected intraperitoneally with LPS were more sensitive to LPS-induced septic shock and died at doses that were not lethal for *Pml*$^{-/-}$ mice (Table 2). Histopathological analysis was performed on the liver taken from treated animals 48 hours after LPS administration. Sections from liver tissue of wild-type mice showed signs of fulminant hepatitis. In contrast, the liver from LPS-treated *Pml*$^{-/-}$ mice showed no signs of hepatotoxicity. The reproducibility of these results in 3 different genetic backgrounds (C57BL/6, 129Sv, and 129Sv-mixed) provides evidence for a model where PML is required for the LPS-activated TLR-dependent NF-κB pathway.

IL6 production is reduced in Pml$^{-/-}$ *mouse embryonic fibroblasts*. Clinical and epidemiological data suggest a strong association between inflammation and different types of cancer. In this context, the NF-κB–dependent release of inflammatory molecules represents important antiapoptotic and growth signals for cancer cells, promoting tumorigenesis and tumor progression.[36,37] Although widely accepted, detailed mechanisms necessary to disentangle the key components of this protumorigenic signaling transduction cascade are still lacking. Among all the cytokines and chemokines normally involved in the inflammatory response, IL6 seems to play a key role in malignant transformation. This cytokine has been implicated as a growth factor for multiple myeloma, epithelial tumors such as breast and prostate cancers, and Hodgkin lymphoma.[38-40] Recently, Struhl and colleagues have described the complex oncogenic mechanism that links an inflammatory stimulus through NF-κB/Lin28B/Let-7/IL6/Stat3 to cellular transformation.[23] In particular, the ability of Let-7 to bind the 3′UTR of IL6 mRNA and to repress its expression is completely lost during an inflammatory stimulus as a consequence of NF-κB–dependent induction of Lin28B. The final result of NF-κB activation is an early and extremely high up-regulation of IL6 in comparison to other inflammation-related genes, which in turn mediates the activation of fundamental oncogenic pathways such as JAK/STAT, VEGF, IL8, IL1A, and IL1B.

In order to determine whether PML could regulate the NF-κB/IL6 inflammatory oncogenic network described above, we quantitated IL6 production in the supernatant of *Pml*$^{-/-}$ and wild-type C57BL/6–derived mouse embryonic fibroblasts (MEFs). In LPS-treated MEFs, IL6 concentration was found to be on average 2-fold higher in the supernatant of wild-type with respect to *Pml*$^{-/-}$ MEF (Fig. 3). These data reinforce the hypothesis that PML might be an important player in the NF-κB pathway and at the same

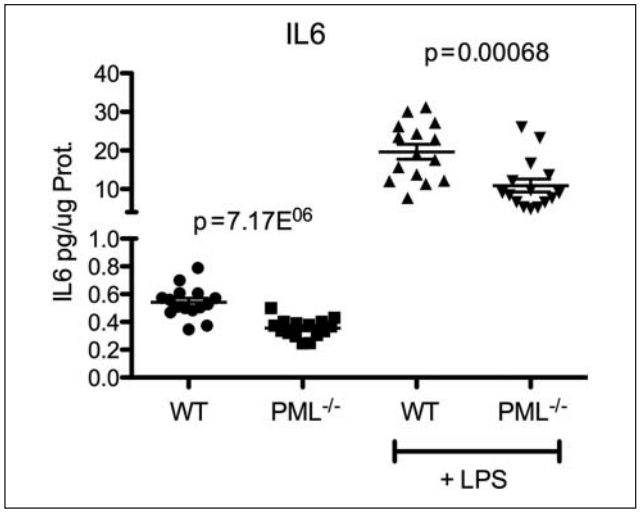

Figure 3. Impaired IL6 production in *Pml*$^{-/-}$ MEFs. Secreted IL6 was measured in the medium by ELISA and is expressed relative to total protein content of incubated MEFs. Five independent experiments showed a statistically significant 2-fold decrease of IL6 protein secretion from *Pml*$^{-/-}$ versus wild-type MEFs after LPS treatment. The mean values are presented by the solid lines ± standard deviation.

time highlight a possible and unexpected proto-oncogenic unrecognized side of this gene in tumors where inflammation is involved.

Discussion

BTM is rare in humans, although it does have a worldwide occurrence, and it is associated with the presence of commensal microorganisms such as *Actinomycetes* and *Staphylococcus*.[27,28] *Pml*$^{-/-}$ mice develop BTM with high penetrance and die from BTM in almost 30% of cases by their first year of age. By year 2, 100% of *Pml*$^{-/-}$ mice show either overt BTM or BTM-type lesions at postmortem analysis. In these mice, the spontaneous infections were characterized by the accumulation of lipochrome histiocytes. The presence of these cells is associated with a group of inherited diseases, chronic granulomatous disease, characterized by impaired macrophage function and susceptibility to infections but not by botryomicosis.[29] The presence of lipochrome histiocytes in the *Pml*$^{-/-}$ mutants, the fact that PML is specifically up-regulated by interferons and is also up-regulated in functionally activated macrophages as well as in germinal center macrophages,[41] prompted us to challenge the mice with *Listeria monocytogenes*. This microorganism replicates in the cytoplasm of macrophages and is killed by these cells once they became activated by various cytokines including interferons.[32] *Pml*$^{-/-}$ mice revealed an impaired capacity to clear *Listeria* infection, once again supporting the notion of altered macrophage function in these mice. The "activated" macrophage is the primary host cell mediating immunity to *Listeria monocytogenes*, while migration of macrophages to the site of *Listeria* replication, phagocytosis, and intracellular killing represent important mechanisms for the eradication of *Listeria*. *Pml*$^{-/-}$ macrophages can migrate into the peritoneal cavity in response to various stimuli and can phagocytose but are not properly activated upon exposure to *Listeria*. Lack of "activation" together with the concomitant altered digestion of the phagocytosed material due to the reduced number of lysosomes, as also shown by the accumulation of lipids in macrophages, explains the immune response defect underlying the spontaneous occurrence of the botryomycotic granuloma. *Pml*$^{-/-}$ macrophages are capable of producing NO upon exposure to LPS and interferons, indicating that PML is not implicated in controlling the transcriptional activation of the iNOS genes induced by LPS and IFNs.

The hyperproliferative response observed in infected *Pml*$^{-/-}$ mice can be experimentally reproduced when the mice are challenged, either locally or systemically, with infectious agents. PML's dual role in controlling cell proliferation as well as the functional activation of macrophages would explain why *Pml* mutants preferentially develop such an unusual lesion as BTM through a combined mechanism of hyperproliferation, impaired clearance, and bacterial trapping, at the same time disclosing the pathogenetic and predisposing factors that result in this rare condition.

In this regard, it is interesting to note that some pathogens are able to escape the acute immune response and establish a persistent infection responsible for a low-grade chronic inflammation. This asymptomatic pathological status has been recently linked to different phases of tumor development in malignancies such as cervical cancer, hepatocellular carcinoma, lymphoproliferative disorders, and gastric tumors, respectively, due to chronic infection by human papilloma virus (HPV), hepatitis B and C viruses (HBV, HCV), Epstein-Barr virus (EBV), and *Helicobacter pylori*.[21] In the majority of these cases, the crucial tumorigenic factor is the chronic inflammation more than the activation of a specific pathogen's oncogenes. In particular, mature T cells and tumor-associated macrophages (TAMs) are the 2 classes of immune cells most frequently found associated with solid tumors. Both cell types are involved in tumor initiation and progression through cytokines (IL1, IL6, IL17, IL23, and TNF-α) and proangiogenic (VEGF) and prometastatic (EGF, TGF-β) factors release.

The NF-κB signaling pathway has emerged as the central node that links, at the molecular level, inflammation and tumorigenesis.[23,42] The IKK/NF-κB system plays multiple roles in this particular game: 1) it can promote cellular transformation; 2) it is able to trigger survival pathways in tumor cells, counteracting proapoptotic stimuli; 3) it drives

the synthesis and release of cytokines and growth factors in the immune cells that are necessary for tumor development and invasiveness.

By using a mouse model of colitis-associated colorectal cancer in which the gene encoding IKKβ, essential for the activation of the NF-κB pathway, was knocked out in either myeloid or intestinal epithelial cells, Greten and colleagues set out the conditions to discern the different cell-dependent contributions of the NF-κB pathway to the inflammation-related tumor development. IKKβ knockout in the intestinal epithelial cells determined an 80% decrease in tumor incidence versus only 50% when the NF-κB pathway was affected in the macrophages.[24] Although the exact mechanism of the noncell-autonomous role in macrophages remained unclear, a cell-autonomous NF-κB–dependent suppression of the mitochondrial apoptosis through the induction of its target gene Bcl-X_L has been proposed. Support for NF-κB's antiapoptotic role in inflammation-driven tumorigenesis came from studies on *Mdr2* knockout mice, a faithful model of hepatitis and hepatocellular carcinoma. Through the genetic alteration of IκBα, an important inhibitor of the NF-κB pathway, Pikarsky and colleagues characterized a fundamental antiapoptotic function of NF-κB in the transformed hepatocytes necessary for the progression to the hepatocellular carcinoma.[25]

Intriguingly, all the phenotypes described in *Pml*$^{-/-}$ mice, including defects in macrophage activation, deregulation of cytokine/chemokine expression, altered response to LPS, and cellular hyperproliferation, are reminiscent of and could be potentially attributed to a dysfunction of the NF-κB pathway. In this regard, the detailed analysis of the role of PML in the modulation of the NF-κB pathway represents an exciting challenge for future studies, not only to further define the role of PML in the innate immune response but also to ascertain a possible unanticipated proto-oncogenic function for PML in chronic inflammation-driven tumor development.

Materials and Methods

Pml$^{-/-}$ *mice*. *Pml*$^{-/-}$ mice were previously generated.[43] All mouse work was performed in accordance with our IACUC-approved protocols.

Autopsy, histopathology, and immunohistochemistry of mice. Animals were autopsied as needed, and all tissues were examined regardless of their pathological status. Tissues were formalin fixed, dehydrated, and embedded in paraffin according to standard protocols. Sections (4-5 μm) were stained with hematoxylin and eosin and examined microscopically. Standard Gram and GMS staining procedures were carried out in order to characterize the microorganisms in the botryomycotic lesion.

Staphylococcus aureus and Listeria monocytogenes infections. For local and systemic infection with *Staphylococcus* subspecies, *aureus* (ATCC 25923) was utilized. 5×10^8 cfu of bacteria resuspended in 300 μL of PBS were injected intraperitoneally into 8 controls and 8 *Pml*$^{-/-}$ 8- to 12-week-old mice. Histopathological analysis was carried out when spontaneous death occurred. 5×10^7 cfu of *Staphylococcus aureus* were injected into the left lobe of the submandibular salivary gland of six 8- to 12-week-old *Pml*$^{-/-}$ and 6 control mice. Animals were sacrificed after 10 days, and postmortem histopathological analysis was performed. For the *Listeria* infections, mice were injected intravenously with 10^4 cfu of *Listeria monocytogenes* (ATCC 7302). The number of viable bacteria recovered from the spleen and the liver was determined 6 days after the injection or immediately after spontaneous death occurred by plating serial 10-fold dilutions of organ homogenates in PBS on trypticase soy agar plate. Three independent experiments were carried out using 4 *Pml*$^{-/-}$ and 4 wild-type mice for each experiment.

Preparation of untreated resident macrophages or thioglycollate or proteose peptone–elicited peritoneal macrophages. Mice were sacrificed 3 days after intraperitoneal injection of 2 mL of 3% Brewer thioglycollate medium or 4 days after intraperitoneal injection of 2 mL of 10% proteose peptone. Resident macrophages were also harvested from untreated mice. Peritoneally exudated cells were harvested by washing the peritoneal cavity with 5 mL of RPMI medium. The cells were cultured for 2 hours in LPS-free RPMI 1640, 10% FCS, 2 mM L-glutamine, penicillin G (100 U/mL), and streptomycin (100 μg/mL). Nonadherent cells were removed, and the remaining macrophage monolayer was used for further experiments.

Transmission electron microscopy of peritoneal macrophages infected with Listeria monocytogenes. Wild-type and *Pml*$^{-/-}$ mice were injected intraperitoneally with 10^7 cfu of *Listeria monocytogenes* resuspended in RPMI 10% FCS. Fifteen minutes later, peritoneal cells were harvested and stained with Wright staining for morphological analysis or fixed with 3% formaldehyde and 3% glutaraldehyde in 0.1 M Miloning's phosphate buffer. The cells were then sectioned and examined with a Philips model 410EM transmission electron microscope (Amsterdam, the Netherlands).

NBT reaction. There was 50 μL of peripheral blood from 4 *Pml*$^{-/-}$ and 4 wild-type control mice added to 50 μL of NBT solution (1 mg of nitroblue tetrazolium per mL of PBS) in a siliconized vial, with or without bacterial extract (Sigma-Aldrich, St. Louis, MO). After 10 minutes at 37 °C, cells were transferred onto a clean glass slide. The positive cells were scored by microscopy. At least 400 cells per mouse were scored.

Nitric oxide production by macrophages. Resident untreated macrophages were collected from both wild-type and $Pml^{-/-}$ mice and plated on a 96-well plate at a density of 1 $\times 10^5$ cells/well. Adherent cells were cultured with or without 100 U/mL IFNγ, 100 ng/mL LPS, or both IFNγ and LPS for 24 or 48 hours. NO concentration in the medium was measured with Griess reagent.[44]

LPS treatment. LPS (L-3129) was purchased from Sigma-Aldrich. Mice were injected intraperitoneally with, respectively, 5 mg (129Sv and 129Sv-mixed) and 1 mg (C57BL/6) of reagents dissolved in 0.1 mL of phosphate-buffered saline.

IL6 quantification by ELISA. An equal amount of primary MEFs derived from wild-type ($n = 3$) and $Pml^{-/-}$ ($n = 3$) C57BL/6 mice was seeded 12 hours before treatment in DMEM containing 10% FBS and 2 mM glutamine. Supernatants from wild-type and $Pml^{-/-}$ MEFs untreated or challenged with 100 ng/mL LPS for 24 hours were analyzed for IL6 by using a commercially available murine IL6 ELISA kit (Thermo Scientific EM2IL6, Waltham, MA) according to the manufacturer's recommendations. IL6 values were normalized to total amount of proteins isolated from wild-type and $Pml^{-/-}$ MEFs, respectively.

Statistical analysis. Results are expressed as mean ± standard deviation. Comparisons between groups were assessed using Student *t* test analysis (Excel, Microsoft, Redmond, WA). $P \leq 0.05$ was considered significant.

Acknowledgments

The authors thank all the members of the Pandolfi laboratory and in particular L. Longo and A. Carracedo Pérez for discussion and comments; S. Nicolis and A. Dejean for suggestions and help with some experiments; J. Rosai for advice on the pathological examination of the mice; D. Sylvestre for the *Listeria monocytogenes*; the Department of Microbiology of MSKCC; and R. Erlandson for the electron microscopy analysis.

Declaration of Conflicting Interests

The author(s) declared no potential conflicts of interest with respect to the authorship and/or publication of this article.

Funding

This work was supported by the Sloan-Kettering Institute and the National Institutes of Health [grant number RO1 CA 71692] awarded to P.P.P.

References

1. Bernardi R, Papa A, Pandolfi PP. Regulation of apoptosis by PML and the PML-NBs. Oncogene. 2008;27:6299-312.
2. Salomoni P, Pandolfi PP. The role of PML in tumor suppression. Cell. 2002;108:165-70.
3. Lin HK, Bergmann S, Pandolfi PP. Cytoplasmic PML function in TGF-beta signalling. Nature. 2004;431:205-11.
4. Bernardi R, Pandolfi PP. Structure, dynamics and functions of promyelocytic leukaemia nuclear bodies. Nat Rev Mol Cell Biol. 2007;8:1006-16.
5. Shen TH, Lin HK, Scaglioni PP, Yung TM, Pandolfi PP. The mechanisms of PML-nuclear body formation. Mol Cell. 2006;24:331-9.
6. Scaglioni PP, Yung TM, Cai A. CK2-dependent mechanism for degradation of the PML tumor suppressor. Cell. 2006;126:269-83.
7. Trotman LC, Alimonti A, Scaglioni PP*, et al*. Identification of a tumour suppressor network opposing nuclear Akt function. Nature. 2006;441:523-7.
8. Alcalay M, Tomassoni L, Colombo E*, et al*. The promyelocytic leukemia gene product (PML) forms stable complexes with the retinoblastoma protein. Mol Cell Biol. 1998;18:1084-93.
9. Bernardi R, Scaglioni PP, Bergmann S, Horn HF, Vousden KH, Pandolfi PP. PML regulates p53 stability by sequestering Mdm2 to the nucleolus. Nat Cell Biol. 2004;6:665-72.
10. Bernardi R, Guernah I, Jin D*, et al*. PML inhibits HIF-1alpha translation and neoangiogenesis through repression of mTOR. Nature. 2006;442:779-85.
11. Trotman LC, Wang X, Alimonti A*, et al*. Ubiquitination regulates PTEN nuclear import and tumor suppression. Cell. 2007;128:141-56.
12. Gurrieri C, Capodieci P, Bernardi R*, et al*. Loss of the tumor suppressor PML in human cancers of multiple histologic origins. J Natl Cancer Inst. 2004;96:269-79.
13. Regad T, Bellodi C, Nicotera P, Salomoni P. The tumor suppressor Pml regulates cell fate in the developing neocortex. Nat Neurosci. 2009;12:132-40.
14. Ito K, Bernardi R, Morotti A*, et al*. PML targeting eradicates quiescent leukaemia-initiating cells. Nature. 2008;453:1072-8.
15. Geoffroy MC, Chelbi-Alix MK. Role of promyelocytic leukemia protein in host antiviral defense. J Interferon Cytokine Res. 2011;31:145-58.
16. Gialitakis M, Arampatzi P, Makatounakis T, Papamatheakis J. Gamma interferon-dependent transcriptional memory via relocalization of a gene locus to PML nuclear bodies. Mol Cell Biol. 2010;30:2046-56.
17. Everett RD, Chelbi-Alix MK. PML and PML nuclear bodies: implications in antiviral defence. Biochimie. 2007;89:819-30.
18. Nisole S, Stoye JP, Saib A. TRIM family proteins: retroviral restriction and antiviral defence. Nat Rev Microbiol. 2005;3:799-808.
19. Carpenter S, O'Neill LA. Recent insights into the structure of Toll-like receptors and post-translational modifications of their associated signalling proteins. Biochem. 2009;J422:1-10.
20. Karin M. NF-kappaB as a critical link between inflammation and cancer. Cold Spring Harb Perspect Biol. 2009;1:a000141.
21. Karin M, Lawrence T, Nizet V. Innate immunity gone awry: linking microbial infections to chronic inflammation and cancer. Cell. 2006;124:823-35.
22. DeNardo DG, Barreto JB, Andreu P*, et al*. CD4(+) T cells regulate pulmonary metastasis of mammary carcinomas by enhancing protumor properties of macrophages. Cancer Cell. 2009;16:91-102.
23. Iliopoulos D, Hirsch HA, Struhl K. An epigenetic switch involving NF-kappaB, Lin28, Let-7 MicroRNA, and IL6 links inflammation to cell transformation. Cell. 2009;139:693-706.

24. Greten FR, Eckmann L, Greten TF*, et al*. IKKbeta links inflammation and tumorigenesis in a mouse model of colitis-associated cancer. Cell. 2004;118:285-96.
25. Pikarsky E, Porat RM, Stein I*, et al*. NF-kappaB functions as a tumour promoter in inflammation-associated cancer. Nature. 2004;431:461-6.
26. Hagemann T, Biswas SK, Lawrence T, Sica A, Lewis CE. Regulation of macrophage function in tumors: the multifaceted role of NF-kappaB. Blood. 2009;113:3139-46.
27. Neafie RC, Marty AM. Unusual infections in humans. Clin Microbiol Rev. 1993;6:34-56.
28. Ahdoot D, Rickman LS, Haghighi P, Heard WU. Botryomycosis in the acquired immunodeficiency syndrome. Cutis. 1995;55:149-52.
29. Dinauer MC, Orkin SH. Chronic granulomatous disease. Annu Rev Med. 1992;43:117-24.
30. Pollock JD, Williams DA, Gifford MA. Mouse model of X-linked chronic granulomatous disease, an inherited defect in phagocyte superoxide production. Nat Genet. 1995;9:202-9.
31. Rodey GE, Park BH, Ford DK, Gray BH, Good RA. Defective bactericidal activity of peripheral blood leukocytes in lipochrome histiocytosis. Am J Med. 1970;49:322-7.
32. Kaufmann SH, Ladel CH. Role of T cell subsets in immunity against intracellular bacteria: experimental infections of knock-out mice with Listeria monocytogenes and Mycobacterium bovis BCG. Immunobiology. 1994;191:509-19.
33. Adams DO, Hamilton TA. Molecular transductional mechanisms by which IFN gamma and other signals regulate macrophage development. Immunol Rev. 1987;97:5-27.
34. Zucker-Franklin D, Seremetis S, Zheng ZY. Internalization of human immunodeficiency virus type I and other retroviruses by megakaryocytes and platelets. Blood. 1990;75:1920-3.
35. Tanaka T, Akira S, Yoshida K. Targeted disruption of the NF-IL6 gene discloses its essential role in bacteria killing and tumor cytotoxicity by macrophages. Cell. 1995;80:353-61.
36. Naugler WE, Karin M. NF-kappaB and cancer-identifying targets and mechanisms. Curr Opin Genet Dev. 2008;18:19-26.
37. Pierce BL, Ballard-Barbash R, Bernstein L. Elevated biomarkers of inflammation are associated with reduced survival among breast cancer patients. J Clin Oncol. 2009;27:3437-44.
38. Kawano M, Hirano T, Matsuda T. Autocrine generation and requirement of BSF-2/IL-6 for human multiple myelomas. Nature. 1998;332:83-5.
39. Nagel S, Scherr M, Quentmeier H. HLXB9 activates IL6 in Hodgkin lymphoma cell lines and is regulated by PI3K signalling involving E2F3. Leukemia. 2005;19:841-6.
40. Sasser AK, Sullivan NJ, Studebaker AW, Hendey LF, Axel AE, Hall BM. Interleukin-6 is a potent growth factor for ER-alpha-positive human breast cancer. FASEB J. 2007;21:3763-70.
41. Flenghi L, Fagioli M, Tomassoni L*, et al*. Characterization of a new monoclonal antibody (PG-M3) directed against the amino-terminal portion of the PML gene product: immunocytochemical evidence for high expression of PML proteins on activated macrophages, endothelial cells, and epithelia. Blood. 1995;85:1871-80.
42. Razani B, Cheng G. NF-kappaB: much learned, much to learn. Sci Signal. 2010;3:pe29.
43. Wang ZG, Delva L, Gaboli M*, et al*. Role of PML in cell growth and the retinoic acid pathway. Science. 1998;279:1547-51.
44. Ding AH, Nathan CF, Stuehr DJ. Release of reactive nitrogen intermediates and reactive oxygen intermediates from mouse peritoneal macrophages: comparison of activating cytokines and evidence for independent production. J Immunol. 1988;141:2407-12.